atoms

MDPI

Article

Two Photon Processes in an Atom Confined in Gaussian Potential

Sonia Lumb [1,†], Shalini Lumb [2,*,†] and Vinod Prasad [3,†]

1 Department of Physics and Electronics, Rajdhani College, University of Delhi, New Delhi 110015, India; sonia_lumb@hotmail.com
2 Department of Physics, Maitreyi College, University of Delhi, New Delhi 110021, India
3 Department of Physics, Swami Shraddhanand College, University of Delhi, Delhi 110036, India; vprasad@ss.du.ac.in
* Correspondence: shalini_lumb@hotmail.com; Tel.: +91-981-109-2072
† These authors contributed equally to this work.

Academic Editor: James F. Babb
Received: 29 December 2015; Accepted: 5 February 2016; Published: 17 February 2016

Abstract: Transitions of an atom under the effect of a Gaussian potential and loose spherical confinement are studied. An accurate Bernstein-polynomial (B-polynomial) method has been applied for the calculation of the energy levels and radial matrix elements. The transition probability amplitudes, transparency frequencies, and resonance enhancement frequencies for transitions to various excited states have been evaluated. The effect of the shape of confining potential on these spectral properties is studied.

Keywords: transition probability amplitudes; transparency frequency; resonance enhancement frequency; B-polynomials

PACS: 32.30.-r; 32.70.-n; 32.80.-t

1. Introduction

Two-photon spectroscopy has been a valuable tool in the case of atomic and molecular systems, as it provides vital tests of the physical theories in addition to providing a ground to evaluate accurate values of some fundamental constants [1–3]. Recently, two-photon and three-photon absorption processes have attracted much attention in the case of semiconducting heterostructures such as quantum wells, wires, and dots [4–7] and atoms and ions confined in a plasma environment [8–11]. Two-photon and multi-photon absorption in these structures have many potential applications, such as in photonics and in the separation of signal and probe photons [12,13]. The two-photon atomic transitions in hydrogen-like systems have been calculated by Amaro *et al.* [14] by solving the Dirac equation (relativistic case).

In addition, these processes provide an important tool for bioimaging applications [15–17]. As reported by Achtstein *et al.* [4], two-photon imaging enables deep tissue penetration. As in the case of atoms, two photon absorption (TPA) is often used for probing the electronic states of these quantum structures [18]. There have been experimental studies on these aspects of TPA, particularly in the case of atoms as impurities in quantum heterostructures [19–22]. Dakovski and Shan [5] have recently studied the size dependence of TPA in the case of spherical quantum dots. TPA in the case of quantum heterostructures is found to be enhanced as compared to bulk material. Lad *et al.* [23] have shown that TPA in ZnSe and ZnSe/ZnS quantum dots is three magnitudes higher than that of bulk material. Also, CdSe quantum rods have been shown to exhibit four times larger TPA as compared to quantum dots of the same mass [24].

Similar studies have recently been initiated with much vigor in the case of atoms and ions confined in a variety of plasma environments and other confinements [25–36]. Some works on two-photon transitions in atoms or ions employing the Ion-Sphere model [37] for strongly-coupled plasmas were also reported in the literature [34,38,39]. The confinement produces many striking changes in the spectrum of the confining system, such as the phenomenon of continuum lowering and the polarization red shift [3]. In particular, the Gaussian confinement causes drastic changes in the physical properties of a confined atom [26]. The Gaussian confining potential has many applications in modelling of the atoms and molecules confined in a cage of carbon [40]. The purpose of this work is to investigate the effect of Gaussian confinement on the TPA process. In the present case, the system is assumed to be under the effect of loose spherical confinement as well, with the confinement radius set at $r_0 = 50$ a.u. To the best of our knowledge, this is the first study of its kind. In the following section, the theoretical method employed to calculate the spectrum of the present system is described, and the TPA process is discussed. This is followed by discussion of the obtained results.

2. Theory

A hydrogen atom under the effect of Gaussian potential is considered. The atom is supposed to be confined spherically with impenetrable walls, such that the wave functions vanish at the boundary $r = r_0$, where r_0 is assumed to have a fixed value of 50 a.u. This is the case of loose spherical confinement as discussed in earlier texts [25–30]. The energy spectrum and dipole matrix elements of the system have been evaluated by solving the corresponding radial Schrödinger equation with the aim to study the two-photon spectra which refers to the excitation process generated by the simultaneous absorption of two less-energetic photons under sufficiently intense laser illumination. This nonlinear process can occur if the sum of the energies of the two photons is equal to the energy gap between the ground and excited states of the system. The important spectral properties, *viz.*, two-photon transition probability amplitudes (D_2), transparency frequencies (ω_t), and resonance enhancement frequencies (ω_r) [41,42] have been calculated. The variation of these properties with the Gaussian confinement parameters V_0 and σ has been studied. Optical properties like oscillator strength and polarizability had been calculated for a hydrogen atom under the effect of Gaussian potential and loose spherical confinement in our earlier work [26]. The method used for solving the Schrödinger equation is based on Bernstein-polynomials (B-polynomials) and is detailed elsewhere [29–32,43,44]. Only the basic outline of the approach followed for the present work has been mentioned in the following text. Atomic units have been employed throughout this study.

The radial Schrödinger equation for the electron of the Gaussian confined hydrogen atom is given by

$$\left[-\frac{1}{2}\frac{d^2}{dr^2} + \frac{l(l+1)}{2r^2} - \frac{1}{r} - V_0 e^{-r^2/\sigma^2} + V_c(r) \right] U_{nl}(r) = E_{nl} U_{nl}(r) \tag{1}$$

where V_0 represents the depth of potential, σ is a measure of the width of the potential, and $V_c(r)$ is the confinement potential, defined as

$$V_c(r) = \begin{cases} 0 & , \quad r < r_0 \\ \infty & , \quad r \geq r_0 \end{cases}$$

The radial wave function $R_{n,l}(r) = U_{n,l}(r)/r$. $U_{n,l}(r)$ is expanded in B-polynomial basis as

$$U_{nl}(r) = \sum_{i=0}^{n} c_i B_{i,n}(r) \tag{2}$$

where c_is are coefficients of expansion and $B_{i,n}(r)$ are B-polynomials of degree n. The radial Schrödinger Equation (1) can be reduced to a symmetric generalized eigenvalue equation in matrix form, given by

$$(A + F + G)C = EDC, \tag{3}$$

where D is the overlap matrix. The eigenvalues E provide the energy levels, and eigenvectors C are used to calculate the corresponding radial wave functions using Equation (2). The standard Fortran EISPACK library has been used to solve Equation (3).

The two-photon transition probability amplitude, D_2, of a hydrogen atom from initial state $1s$ to final state js is evaluated using [9,45]

$$D_2 = \frac{1}{2}\sum_n \left[\frac{1}{-E_{1s} + E_n - \omega_0} + \frac{1}{-E_{js} + E_n + \omega_0}\right]\chi^n_{1s}\chi^n_{js} \tag{4}$$

where n represents the intermediate states including continuum, E_{1s} and E_{js} are the energies of $1s$ and js states, respectively, and χ^n_{1s} and χ^n_{js} are the dipole matrix elements evaluated using the expression

$$\chi^n_k = \int_0^\infty r^3 R_n R_k dr, \qquad (k = 1, j) \tag{5}$$

where R_l (with $l = n, k$) is the radial wave function. The corresponding transition probability amplitude for $1s$ to jd state is calculated using

$$D_2 = \frac{1}{\sqrt{5}}\sum_n \left[\frac{1}{-E_{1s} + E_n - \omega_0} + \frac{1}{-E_{jd} + E_n + \omega_0}\right]\chi^n_{1s}\chi^n_{jd} \tag{6}$$

The incident photon frequencies lying in the interval $\Delta E_{if}/2$ and ΔE_{if}, where ΔE_{if} is the difference between final and initial ($1s$) state energies, and for which D_2 approaches infinity, are defined as the resonance enhancement frequencies [9]. The frequencies for which transition amplitude vanishes are the two-photon transparency frequencies [9]. The data for the transition probability amplitudes calculated using Equations (4) and (6) for different confinement conditions reflect the corresponding transparency and resonance enhancement frequencies.

3. Results and Discussion

The effect of the Gaussian confinement parameters V_0 and σ, representing well depth and width, respectively, on the two-photon transition probability amplitudes for a hydrogen atom confined in Gaussian potential is explored. The atom is assumed to be confined within an impenetrable spherical boundary of radius $r_0 = 50$ a.u. This constitutes a loosely-bound system as mentioned in Section 2. This fact has also been established by performing the calculations for $r_0 = 40$ a.u. Some of the corresponding results have been presented at the end of Section 3. The probability amplitudes from $1s$ to js ($j = 2,3,4$) and jd ($j = 3,4$) states have been calculated using Equations (4) and (6), respectively, for different incident photon frequencies that are assumed to lie in the interval $\Delta E_{i,f}/2$ to $\Delta E_{i,f}$. This range of frequencies is a function of both V_0 and σ, since the calculated energy spectrum is dependent on these parameters [26]. The selected range is found to shift towards higher frequencies with an increase in both V_0 and σ. As a check on our calculations, we have matched some of our results with those available in the literature for the case of a free hydrogen atom. The values of $|D_2|$ calculated in the present case for $V_0 = 0$ have been compared with those reported by Paul and Ho [45] in Table 1.

Figures 1–5 depict the variation of the probability amplitudes with V_0 and σ for $1s \rightarrow 2s$, $1s \rightarrow 3s$, $1s \rightarrow 4s$, $1s \rightarrow 3d$, and $1s \rightarrow 4d$ transitions, respectively. In order to demonstrate the effect of these parameters, only two values of V_0 and σ have been selected for pictorial representation of the results. Our results should be experimentally relevant, since the range of values of the Gaussian confinement parameters selected for studying the two photon processes in the present work approximately overlaps the range of values taken by Nascimento *et al.* [40]. In Figures 1–5,

the panel on the left corresponds to $\sigma = 1$ a.u. and the panel on the right corresponds to $\sigma = 5$ a.u. The top panel corresponds to $V_0 = 0.2$ a.u., whereas the bottom panel corresponds to $V_0 = 0.4$ a.u. From this graphical representation of two photon transition probability amplitudes, the nature of the curves is, in general, found to depend on both of these parameters. The resonance enhancement feature is easily discernible from these curves. It is evident from Figures 1–5 that with an increase in either V_0 or σ (keeping the other parameter fixed), the resonance enhancement frequency is more sharply defined. In other words, the linewidth of the resonance curves, signifying the means of determining the lifetimes of resultant states, is a function of the confinement parameters. For example, the resonance at $\omega_0 = 1.5$ a.u. in Figure 3d is rather narrow, whereas one at $\omega_0 = 0.85$ a.u. in Figure 4a is comparatively broad.

Table 1. Comparison of $|D_2|$ for free hydrogen with results available in [45].

$\omega_0(Ryd.)$	$\|D_2\|$ $(1s \rightarrow 2s)$		$\|D_2\|$ $(1s \rightarrow 3s)$	
	Present Study	**Reference [45]**	**Present Study**	**Reference [45]**
0.3750	11.780338	11.7805	3.235425	3.2354
0.5250	14.731690	14.7319		
0.6750	41.147800	41.1484	1.669316	1.6693
0.6875	49.686983	49.6878	0.696330	0.6963
0.7000	62.658358	62.6595	0.984604	0.9847
0.7125	84.523402	84.5252	4.158088	4.1583
0.7250	128.680019	128.6835	11.215759	11.2162
0.7375	262.153248	262.1654	34.224314	34.2263
0.7475	1334.059059	1334.3261	226.765862	226.8138
0.7650			58.200900	58.2000
0.8000			38.309623	38.3099
0.8250			46.579090	46.5797
0.8500			74.418968	74.4204
0.8750			219.974861	219.9847
0.8860			1117.033823	1117.2380

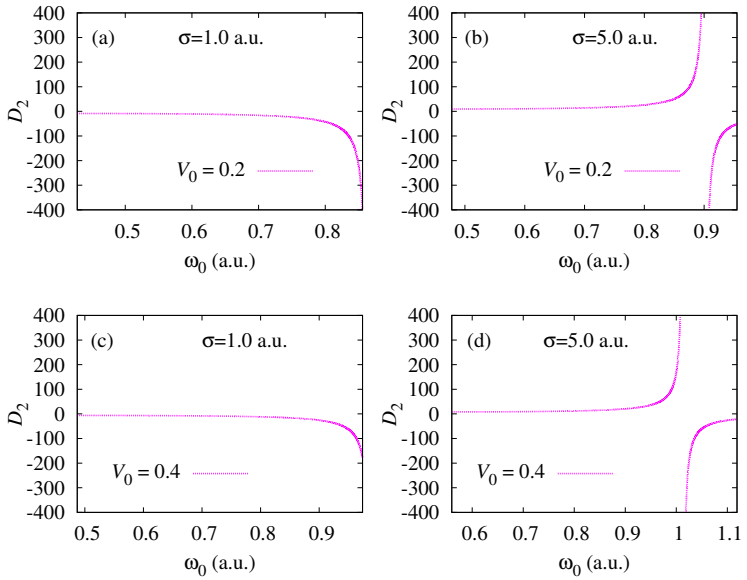

Figure 1. Variation of two-photon $1s \rightarrow 2s$ transition probability amplitude with frequency of incoming photons, ω_0, for (**a**) $V_0 = 0.2$ a.u. and $\sigma = 1.0$ a.u.; (**b**) $V_0 = 0.2$ a.u. and $\sigma = 5.0$ a.u.; (**c**) $V_0 = 0.4$ a.u. and $\sigma = 1.0$ a.u.; (**d**) $V_0 = 0.4$ a.u. and $\sigma = 5.0$ a.u.

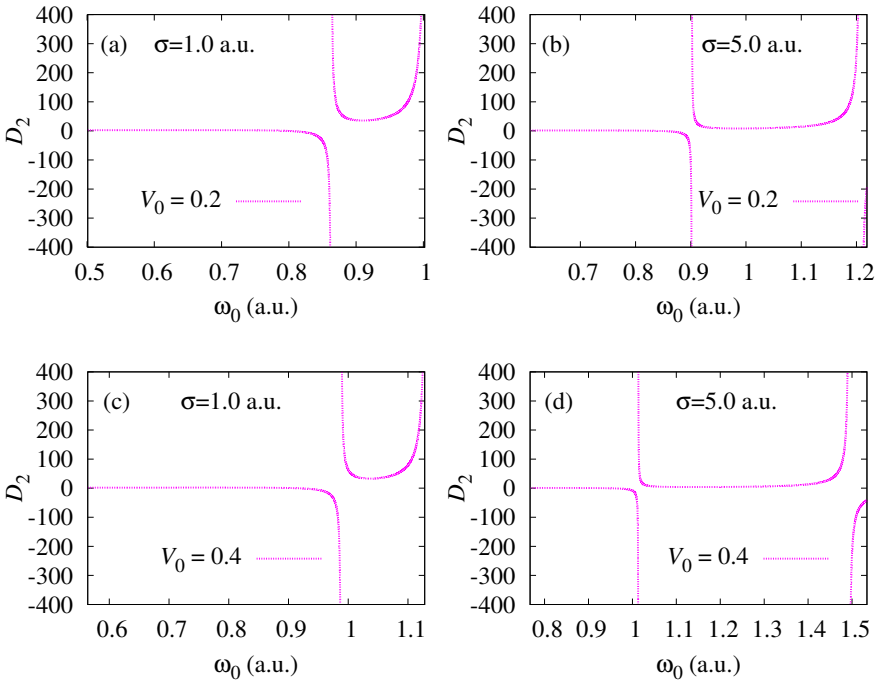

Figure 2. Variation of two-photon $1s \rightarrow 3s$ transition probability amplitude with frequency of incoming photons, ω_0, for (**a**) $V_0 = 0.2$ a.u. and $\sigma = 1.0$ a.u.; (**b**) $V_0 = 0.2$ a.u. and $\sigma = 5.0$ a.u.; (**c**) $V_0 = 0.4$ a.u. and $\sigma = 1.0$ a.u.; (**d**) $V_0 = 0.4$ a.u. and $\sigma = 5.0$ a.u.

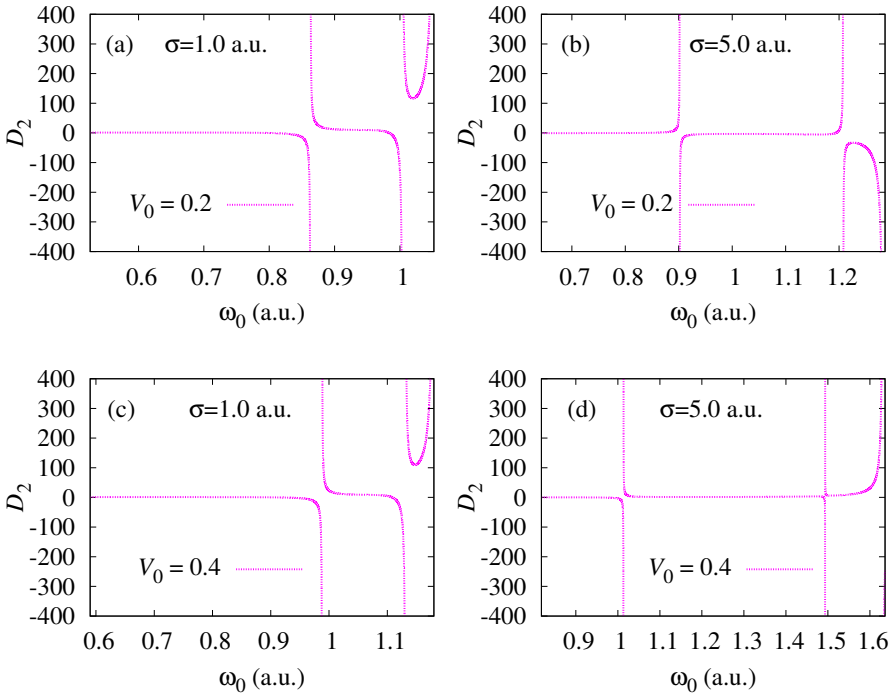

Figure 3. Variation of two-photon $1s \rightarrow 4s$ transition probability amplitude with frequency of incoming photons, ω_0, for (**a**) $V_0 = 0.2$ a.u. and $\sigma = 1.0$ a.u.; (**b**) $V_0 = 0.2$ a.u. and $\sigma = 5.0$ a.u.; (**c**) $V_0 = 0.4$ a.u. and $\sigma = 1.0$ a.u.; (**d**) $V_0 = 0.4$ a.u. and $\sigma = 5.0$ a.u.

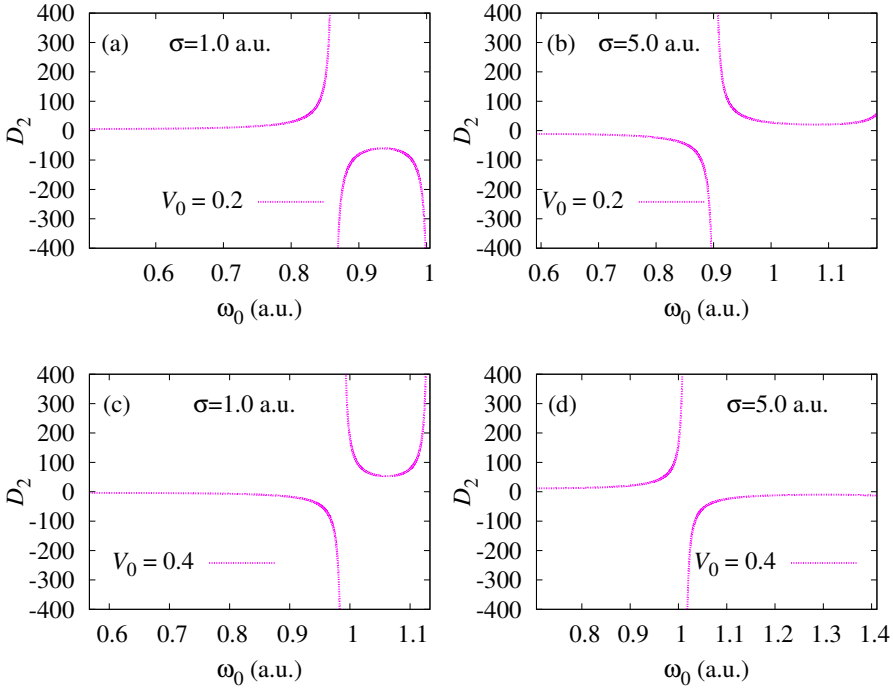

Figure 4. Variation of two-photon $1s \rightarrow 3d$ transition probability amplitude with frequency of incoming photons, ω_0, for (**a**) $V_0 = 0.2$ a.u. and $\sigma = 1.0$ a.u.; (**b**) $V_0 = 0.2$ a.u. and $\sigma = 5.0$ a.u.; (**c**) $V_0 = 0.4$ a.u. and $\sigma = 1.0$ a.u.; (**d**) $V_0 = 0.4$ a.u. and $\sigma = 5.0$ a.u.

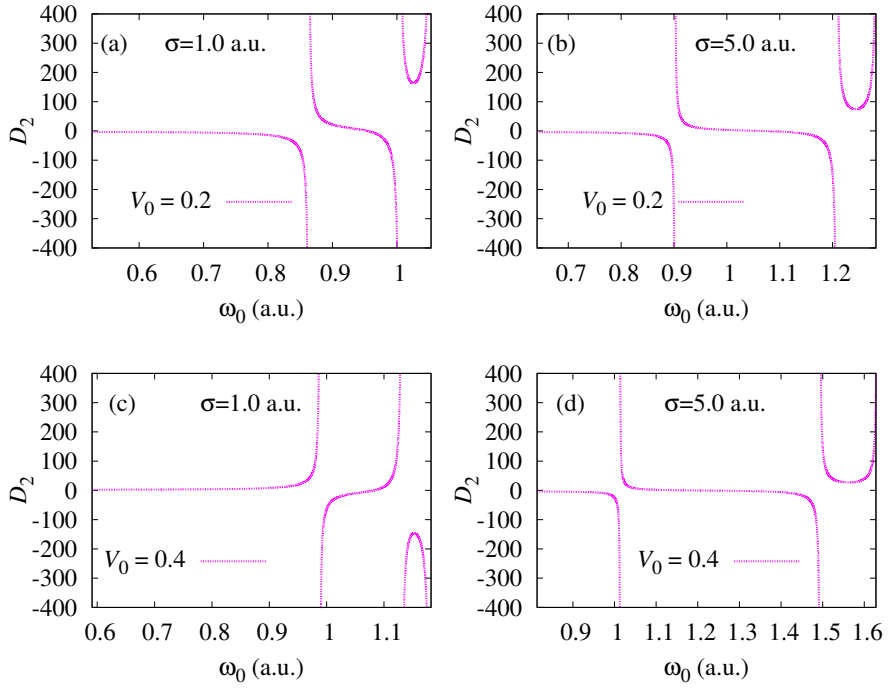

Figure 5. Variation of two-photon $1s \rightarrow 4d$ transition probability amplitude with frequency of incoming photons, ω_0, for (**a**) $V_0 = 0.2$a.u. and $\sigma = 1.0$ a.u.; (**b**) $V_0 = 0.2$ a.u. and $\sigma = 5.0$ a.u.; (**c**) $V_0 = 0.4$ a.u. and $\sigma = 1.0$ a.u.; (**d**) $V_0 = 0.4$ a.u. and $\sigma = 5.0$ a.u.

Figures 1–3 show that for $1s \rightarrow js$ transitions, the number of resonance enhancement frequencies is more for higher values of σ for fixed V_0. For example, for $1s \rightarrow 3s$ transition, there is only one such

frequency for $\sigma = 1$ a.u. as compared to two for $\sigma = 5$ a.u. for both values of V_0. An opposite trend is seen in Figures 4 and 5 for $1s \rightarrow jd$ transitions. It may be mentioned that similar results have been obtained in the context of spherical confinement for a hydrogen atom under Debye potential [46].

Based on the calculated two-photon transition probability amplitudes for V_0 varying from 0.2 a.u. to 1 a.u. and σ from 0.2 a.u. to 5 a.u., the data for two-photon transparency and resonance enhancement frequencies has been tabulated. The transparency frequencies are presented in Table 2 and resonance enhancement frequencies in Tables 3 and 4. The features of transition probability amplitudes discussed above with reference to Figures 1–5 are apparently in consonance with the results presented in Tables 2–4. The data in Tables 3 and 4 also suggest that the positions of the resonance enhancement frequencies shift with change in Gaussian confinement parameters. This fact is related to the changes in the obtained energy spectrum or the bound states. The shifting pattern is observed to be largely similar for the transparency as well as the resonance enhancement frequencies.

Table 2. Two-photon transparency frequencies for various potential widths and depths. The data is in atomic units.

σ	V_0	$1s \rightarrow 3s$	$1s \rightarrow 4s$	$1s \rightarrow 4d$
0.2	0.2	0.6966575	0.6943135	0.8417985
			0.8748915	
	0.4	0.6997875	0.6974305	0.8455535
			0.8784775	
	0.6	0.7029685	0.7005985	0.8493665
			0.8821205	
	0.8	0.7062005	0.7038175	0.8532385
			0.8858195	
	1.0	0.7094835	0.7070865	0.8571695
			0.8895765	
1.0	0.2	0.7966715	0.7946135	0.9540155
			0.9837665	
	0.4	0.9129015	0.9111615	1.0823305
			1.1088085	
	0.6	1.0413755	1.0399605	1.2221895
			1.2456185	
	0.8	1.1810825	1.1799705	1.3726705
			1.3932485	
	1.0	1.3309895	1.3301425	1.5328565
			1.5507545	
2.0	0.2	0.9120575	0.9100275	1.0821115
			1.1100905	
	0.4	1.1385265	1.1359635	1.3399855
			1.3627115	
	0.6	1.3661185	1.3623365	
			1.6253105	
	0.8	1.5894415	1.5839235	1.8820885
			1.8955715	
	1.0	1.8046355	1.7971595	2.1605405
			2.1721445	
5.0	0.2	0.8393165	0.8325805	1.0656265
			1.1942105	
	0.4	0.9385475	0.9232605	1.1849155
			1.4908805	
	0.6	1.0136965	1.7431005	1.2573295
	0.8		1.9660075	
	1.0		1.4822535	
			2.1662075	

Table 3. Two-photon resonance enhancement frequencies for various potential widths and depths. The data is in atomic units.

σ	V_0	$1s \rightarrow 3s$	$1s \rightarrow 4s$	$1s \rightarrow 3d$	$1s \rightarrow 4d$
0.2	0.2	0.7536975	0.7536975	0.7536975	0.7536975
			0.8925875	0.8925875	0.8925875
	0.4	0.7574475	0.7574475	0.7574475	0.7574475
			0.8963405	0.8963405	0.8963405
	0.6	0.7612565	0.7612565	0.7612565	0.7612565
			0.9001505	0.9001505	0.9001505
	0.8	0.7651245	0.7651245	0.7651245	0.7651245
			0.9040205	0.9040205	0.9040205
	1	0.7690515	0.7690515	0.7690515	0.7690515
			0.9079485	0.9079485	0.9079485
1	0.2	0.8630055	0.8630055	0.8630055	0.8630055
			1.0038595	1.0038595	1.0038595
					1.0530765
	0.4	0.9880245	0.9880245	0.9880245	0.9880245
			1.1311185	1.1311185	1.1311185
					1.1809445
	0.6	1.1241155	1.1241155	1.1241155	1.1241155
			1.2697875	1.2697875	1.2697875
					1.3203075
	0.8	1.2702465	1.2702465	1.2702465	1.2702465
			1.4189135	1.4189135	1.4189135
					1.4702285
	1	1.4253685	1.4253685	1.4253685	1.4253685
			1.5775475	1.5775475	1.5775475
					1.6297795

Table 4. Two-photon resonance enhancement frequencies for various potential widths and depths. The data is in atomic units.

σ	V_0	$1s \rightarrow 2s$	$1s \rightarrow 3s$	$1s \rightarrow 4s$	$1s \rightarrow 3d$	$1s \rightarrow 4d$
2	0.2	0.9625345	0.9625345	0.9625345	0.9625345	0.9625345
			1.1264855	1.1264855	1.1264855	1.1264855
				1.1802345		1.1802345
	0.4	1.1717755	1.1717755	1.1717755	1.1717755	1.1717755
			1.3771515	1.3771515	1.3771515	1.3771515
				1.4370505		1.4370505
	0.6	1.3696755	1.3696755	1.3696755	1.3696755	1.3696755
			1.6383765	1.6383765	1.6383765	1.6383765
				1.7046825		1.7046825
	0.8	1.5528565	1.5528565	1.5528565	1.5528565	1.5528565
			1.9086325	1.9086325	1.9086325	1.9086325
				1.9809315		1.9809315
	1	1.7214035	1.7214035	1.7214035	1.7214035	1.7214035
			2.1863955	2.1863955	2.1863955	2.1863955
				2.2641365		2.2641365
5	0.2	0.9017875	0.9017875	0.9017875	0.9017875	0.9017875
			1.2076625	1.2076625		1.2076625
				1.2833555		
	0.4	1.0133065	1.0133065	1.0133065	1.0133065	1.0133065
			1.4933425	1.4933425		1.4933425
				1.6303775		
	0.6	1.1047275	1.1047275	1.1047275	1.1047275	1.1047275
			1.7368975	1.7368975		1.7368975
				1.9763745		
	0.8	1.1844925	1.1844925	1.1844925	1.1844925	1.1844925
			1.9540065	1.9540065		1.9540065
				2.3162335		
	1	1.2556685	1.2556685	1.4262795	1.2556685	1.2749545
			2.1478855	2.1478855		2.1478855
				2.6377985		

A spectrum of energy states has been shown in Table 5 in order to make the interpretation of TPA data easier. This table includes the results for $V_0 = 0$, which corresponds to the case of free hydrogen. The energy levels for $V_0 = 0$ are found to be in agreement with those given by Paul and Ho [45] for $\lambda_D = \infty$.

Table 5. First few energy levels of a hydrogen atom under the effect of a Gaussian potential and loose spherical confinement for $r_0 = 50$ a.u. and for various values of σ and V_0.

n	l	$\sigma(a.u.)$	$V_0 = 0.0(a.u.)$	$V_0 = 0.2(a.u.)$	$V_0 = 0.4(a.u.)$
1	0	1.0	−0.500000	−0.557966	−0.622137
2	0		−0.125000	−0.130189	−0.135136
2	1		−0.125000	−0.126463	−0.128125
3	0		−0.055556	−0.057016	−0.058382
3	1		−0.055556	−0.056037	−0.056578
3	2		−0.055556	−0.055564	−0.055573
4	0		−0.031204	−0.031818	−0.032386
4	1		−0.031216	−0.031428	−0.031665
4	2		−0.031233	−0.031238	−0.031244
4	3		−0.031246	−0.031246	−0.031246
1	0	5.0		−0.679948	−0.861344
2	0			−0.202437	−0.301700
2	1			−0.229055	−0.354691
3	0			−0.070459	−0.094417
3	1			−0.076117	−0.114672
3	2			−0.087940	−0.155671
4	0			−0.036800	−0.043339
4	1			−0.038271	−0.046155
4	2			−0.038904	−0.047266
4	3			−0.033498	−0.044919

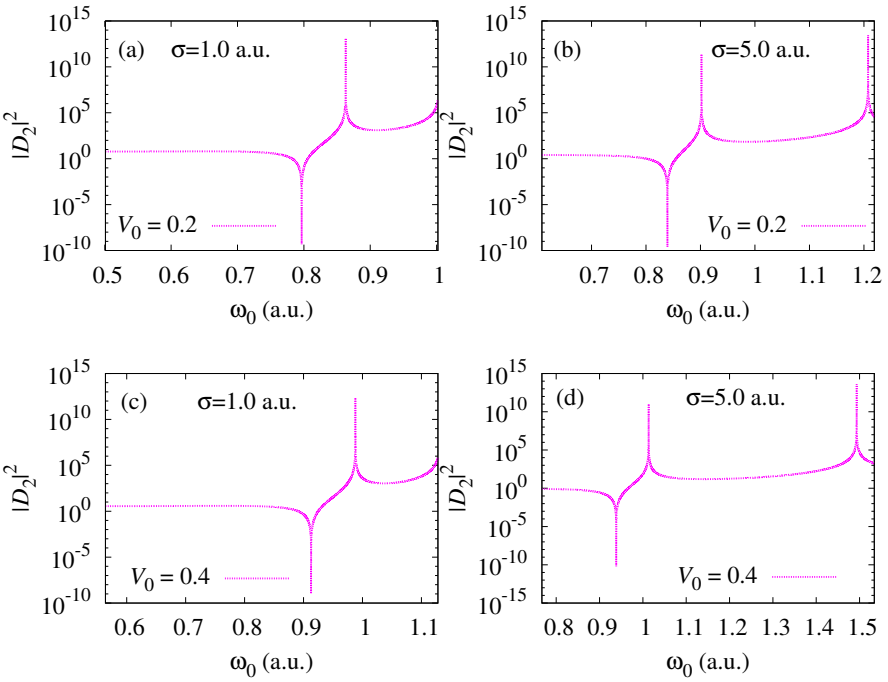

Figure 6. Variation of two-photon $1s \rightarrow 3s$ absorption coefficients with frequency of incoming photons, ω_0, for (**a**) $V_0 = 0.2$ a.u. and $\sigma = 1.0$ a.u.; (**b**) $V_0 = 0.2$ a.u. and $\sigma = 5.0$ a.u.; (**c**) $V_0 = 0.4$ a.u. and $\sigma = 1.0$ a.u.; (**d**) $V_0 = 0.4$ a.u. and $\sigma = 5.0$ a.u.

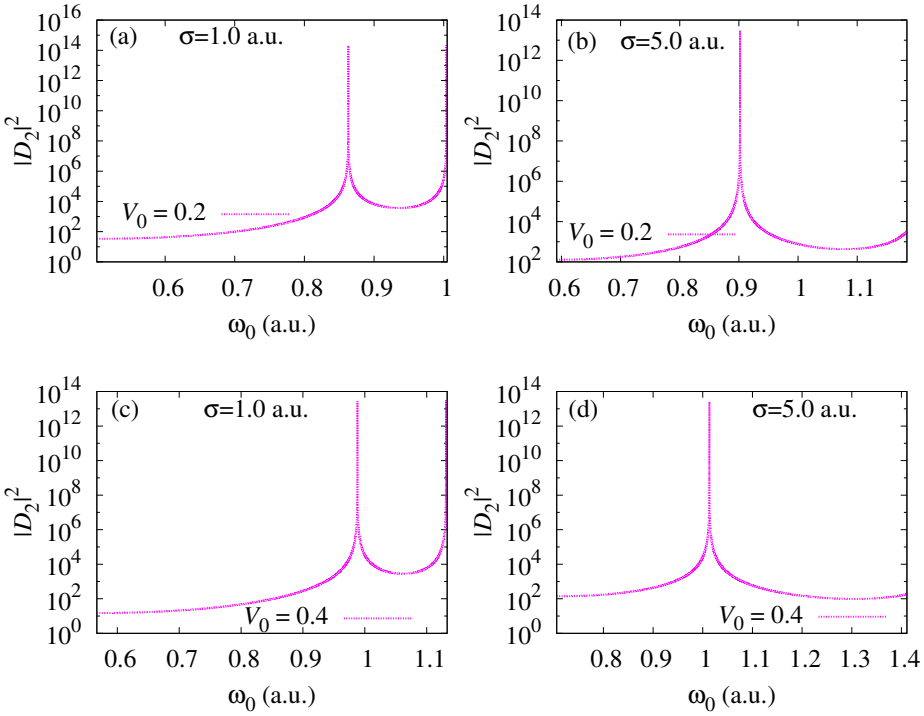

Figure 7. Variation of two-photon $1s \rightarrow 3d$ absorption coefficients with frequency of incoming photons, ω_0, for (**a**) $V_0 = 0.2$ a.u. and $\sigma = 1.0$ a.u.; (**b**) $V_0 = 0.2$ a.u. and $\sigma = 5.0$ a.u.; (**c**) $V_0 = 0.4$ a.u. and $\sigma = 1.0$ a.u.; (**d**) $V_0 = 0.4$ a.u. and $\sigma = 5.0$ a.u.

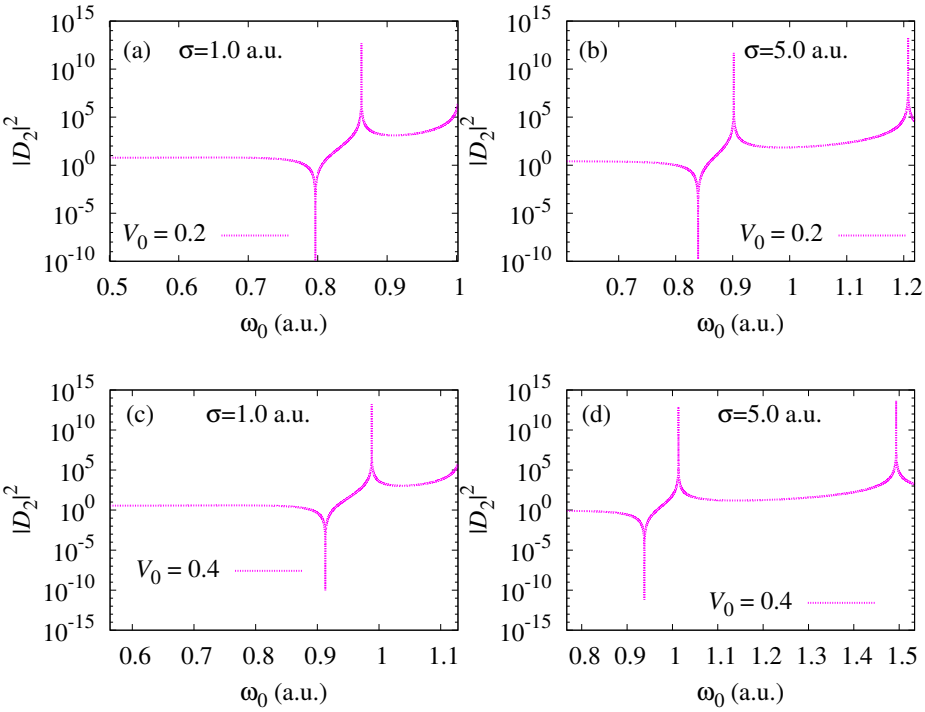

Figure 8. Variation of two-photon $1s \rightarrow 3s$ absorption coefficients with frequency of incoming photons, ω_0, for $r_0 = 40$ a.u. for (**a**) $V_0 = 0.2$ a.u. and $\sigma = 1.0$ a.u.; (**b**) $V_0 = 0.2$ a.u. and $\sigma = 5.0$ a.u.; (**c**) $V_0 = 0.4$ a.u. and $\sigma = 1.0$ a.u.; (**d**) $V_0 = 0.4$ a.u. and $\sigma = 5.0$ a.u.

The two-photon absorption coefficients $|D_2|^2$, which make the study of TPA more comprehensible and relevant to experimental results, have also been calculated and presented in Figures 6 and 7 for the transitions $1s \rightarrow 3s$ and $1s \rightarrow 3d$, respectively, for a better understanding of the results. As can be seen from the figure, the absorption peaks shift with change in any of the Gaussian confinement parameters—*i.e.*, σ or V_0. We understand that this shifting of peaks is due to a change in the energy spectrum of the system, as the energies and corresponding matrix elements vary with both these parameters.

Figures 8 and 9 show the variation of absorption coefficients for $1s \rightarrow 3s$ and $1s \rightarrow 3d$ transitions, respectively, for $r_0 = 40$ a.u. The pattern observed in these figures is nearly same as in Figures 6 and 7 for $r_0 = 50$ a.u. Also, we do not expect much change for $r_0 = 60$ a.u. This refers to the fact that the boundary would not influence the absorption significantly, as r_0 changes from 40 to 60 a.u. This range of r_0 therefore corresponds to a loosely spherically-bound system. However, changing r_0 to small values, say, 10 or 5 a.u., will have a significant effect on the energy spectrum and hence all other properties of the system (not presented in this work).

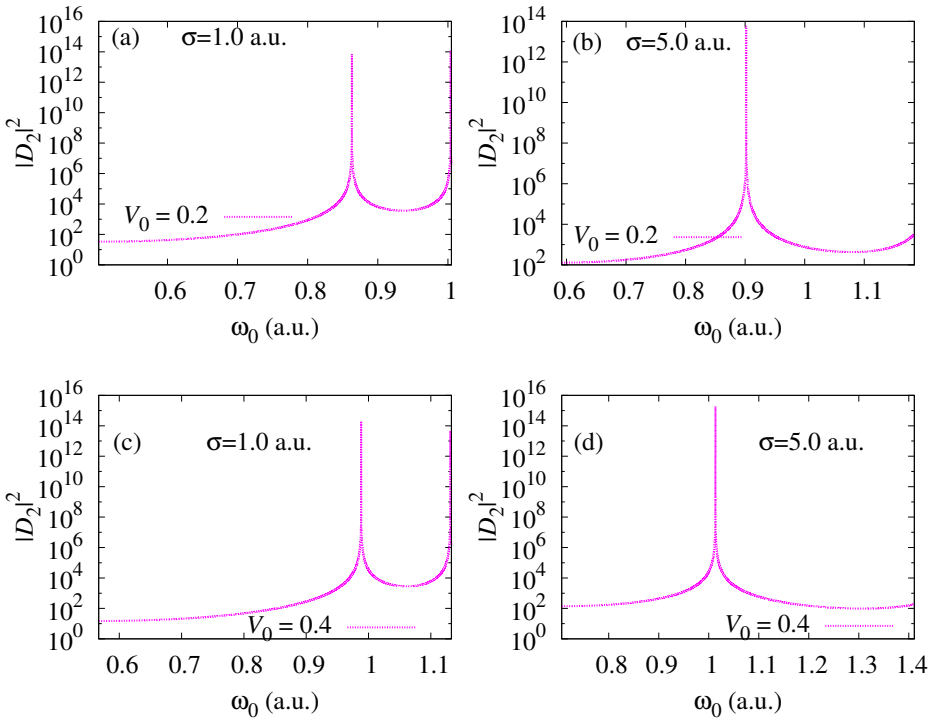

Figure 9. Variation of two-photon $1s \rightarrow 3d$ absorption coefficients with frequency of incoming photons, ω_0, for $r_0 = 40$ a.u. for (**a**) $V_0 = 0.2$ a.u. and $\sigma = 1.0$ a.u.; (**b**) $V_0 = 0.2$ a.u. and $\sigma = 5.0$ a.u.; (**c**) $V_0 = 0.4$ a.u. and $\sigma = 1.0$ a.u.; (**d**) $V_0 = 0.4$ a.u. and $\sigma = 5.0$ a.u.

4. Conclusions

The two-photon transition processes of a hydrogen atom confined by a Gaussian potential have been investigated. The dependence of two-photon transition probability amplitudes, transparency frequencies, and resonance enhancement frequencies on confinement parameters has been explored. With an increase in the depth of Gaussian confinement, more frequencies correspond to resonance enhancement. With an increase in well width, the number of resonance enhancement frequencies has been found to increase for $1s \rightarrow js$, $(j = 2, 3, 4)$ and decrease for $1s \rightarrow jd$, $(j = 3, 4)$ transitions.

Author Contributions: Vinod Prasad suggested the main idea of the paper and helped in interpretation of the results. Calculations were performed by Sonia Lumb and Shalini Lumb. All authors contributed to the writing of the manuscript.

Conflicts of Interest: The authors declare no conflict of interest.

References

1. Kundliya, R.; Prasad, V.; Mohan, M. The two-photon process in an atom using the pseudostate summation technique. *J. Phys. B At. Mol. Opt. Phys.* **2000**, *33*, 5263–5274.
2. Joshi, R. Two-photon transitions to Rydberg states of hydrogen. *Phys. Lett. A* **2007**, *361*, 352–355.
3. Basu, J.; Ray, D. Dynamic polarizability of an atomic ion within a dense plasma. *Phys. Rev. E* **2011**, *83*, 016407.
4. Achtstein, A.W.; Ballester, A.; Movilla, J.L.; Hennig, J.; Climente, J.I.; Prudnikau, A.; Antanovich, A.; Scott, R.; Artemyev, M.V.; Planelles, J.; *et al.* One- and Two- Photon Absorption in CdS Nanodots and Wires: The Role of Dimensionality in the One- and Two-Photon Luminescence Excitation Spectrum. *J. Phys. Chem. C* **2015**, *119*, 1260–1267.
5. Dakovski, G.L.; Shan, J. Size dependence of two-photon absorption in semiconductor quantum dots. *J. App. Phys.* **2013**, *114*, 014301.
6. Khatei, J.; Sandeep, C.S.S.; Philip, R.; Rao, K.S.R.K. Near-resonant two-photon absorption in luminescent CdTe quantum dots. *App. Phys Lett.* **2012**, *100*, 081901.
7. Xia, C.; Spector, H.N. Nonlinear Franz-Keldysh effect: Two photon absorption in semiconducting quantum wires and quantum boxes. *J. App. Phys.* **2009**, *106*, 124302.
8. Paul, S.; Ho, Y.K. Three-photon transitions in the hydrogen atom immersed in Debye plasmas. *Phys. Rev. A* **2009**, *79*, 032714.
9. Paul, S.; Ho, Y.K. Effects of Debye plasmas on two-photon transitions in lithium atoms. *Phys. Rev. A* **2008**, *78*, 042711.
10. Paul, S.; Ho, Y.K. Two-colour three-photon transitions in a hydrogen atom embedded in Debye plasmas. *J. Phys. B At. Mol. Opt. Phys.* **2010**, *43*, 065701.
11. Chang, T.N.; Fang, T.K.; Ho, Y.K. One- and two-photon ionization of hydrogen atom embedded in Debye plasmas. *Phys. Plasmas* **2013**, *20*, 092110.
12. De Wild, J.; Meijerink, A.; Rath, J.K.; van Sarka, W.G.J.H.M.; Schropp, R.E.I. Upconverter solar cells: Materials and applications. *Energy Environ. Sci.* **2011**, *4*, 4835–4848.
13. Lin, Z.; Vučković, J. Enhanced two-photon processes in single quantum dots inside photonic crystal nanocavities. *Phys. Rev. B* **2010**, *81*, 035301.
14. Amaro, P.; Surzhykov, A.; Parente, F.; Indelicato, P.; Santos, J.P. Calculation of two-photon decay rates of hydrogen-like ions by using B-polynomials. *J. Phys. A Math. Theor.* **2011**, *44*, 245302.
15. Prasad, V.; Dahiya, B. Modifications of laser field assisted intersubband transitions in the coupled quantum wells due to static electric field. *Phys. Status Solidi B* **2011**, *248*, 1727–1734.
16. Lahon, S.; Gambhir, M.; Jha, P.K.; Mohan, M. Multiphoton excitation of disc shaped quantum dot in presence of laser (THz) and magnetic field for bioimaging. *Phys. Status Solidi B* **2010**, *247*, 962–967.
17. Larson, D.R.; Zipfel, W.R.; Williams, R.M.; Clark, S.W.; Bruchez, M.P.; Wise, F.W.; Webb, W.W. Water-Soluble Quantum Dots for Multiphoton Fluorescence Imaging *in Vivo*. *Science* **2003**, *300*, 1434–1436.
18. Schmidt, M.E.; Blanton, S.A.; Hines, M.A.; Guyot-Sionnest, P. Size-dependent two-photon excitation spectroscopy of CdSe nanocrystals. *Phys. Rev. B* **1996**, *53*, 12629–12632.
19. Cotter, D.; Burt, M.G.; Manning, R.J. Below-band-gap third-order optical nonlinearity of nanometer-size semiconductor crystallites. *Phys. Rev. Lett.* **1992**, *68*, 1200–1203.
20. Banfi, G.P.; Degiorgio, V.; Ghigliazza, M.; Tan, H.M.; Tomaselli, A. Two-photon absorption in semiconductor nanocrystals. *Phys. Rev. B* **1994**, *50*, 5699–5702.
21. Padilha, L.; Fu, J.; Hagan, D.; van Stryland, E.; Cesar, C.; Barbosa, L.; Cruz, C. Two-photon absorption in CdTe quantum dots. *Opt. Express* **2005**, *13* 6460–6467.
22. Padilha, L.A.; Fu, J.; Hagan, D.J.; van Stryland, E.W.; Cesar, C.L.; Barbosa, L.C.; Cruz, C.H.B.; Buso, D.; Martucci, A. Frequency degenerate and nondegenerate two-photon absorption spectra of semiconductor quantum dots. *Phys. Rev. B* **2007**, *75*, 075325.
23. Lad, A.D.; Kiran, P.P.; More, D.; Kumar, G.R.; Mahamuni, S. Two-photon absorption in ZnSe and ZnSe/ZnS core/shell quantum structures. *App. Phys. Lett.* **2008**, *92*, 043126.

24. Nyk, M.; Szeremeta, J.; Wawrzynczyk, D.; Samoc, M. Enhancement of Two-Photon Absorption Cross Section in CdSe Quantum Rods. *J. Phys. Chem. C* **2014**, *118*, 17914–17921.
25. Lumb, S.; Lumb, S.; Munjal, D.; Prasad, V. Intense field induced excitation and ionization of an atom confined in a dense quantum plasma. *Phys. Scr.* **2015**, *90*, 1–10.
26. Lumb, S.; Lumb, S.; Prasad, V. Static polarizability of an atom confined in Gaussian potential. *Eur. Phys. J. Plus* **2015**, *130*, 149–160.
27. Lumb, S.; Lumb, S.; Prasad, V. Photoexcitation and ionization of hydrogen atom confined in Debye environment. *Eur. Phys. J. D* **2015**, *69*, 176–184.
28. Lumb, S.; Lumb, S.; Prasad, V. Photoexcitation and ionization of a hydrogen atom confined by a combined effect of a spherical box and Debye plasma. *Phys. Lett. A* **2015**, *379*, 1263–1269.
29. Lumb, S.; Lumb, S.; Prasad, V. Photoionization of confined hydrogen atom by short laser pulses. *Indian J. Phys.* **2015**, *89*, 13–21.
30. Lumb, S.; Lumb, S.; Prasad, V. Laser-induced excitation and ionization of a confined hydrogen atom in an exponential-cosine-screened Coulomb potential. *Phys. Rev. A* **2014**, *90*, 1–9.
31. Lumb, S.; Lumb, S.; Prasad, V. Dynamics of Particle in Confined-Harmonic Potential in External Static Electric Field and Strong Laser Field. *J. Mod. Phys.* **2013**, *4*, 1139–1148.
32. Lumb, S.; Lumb, S.; Prasad, V. Response of a Harmonically Confined System to Short Laser Pulses. *Quantum Matter* **2013**, *2*, 314–320.
33. Salzmann, D. *Atomic Physics in Hot Plasmas*; Oxford University Press: Oxford, UK, 1998.
34. Sen, S.; Mandal, P.; Mukherjee, P.K.; Fricke, B. Hyperpolarizabilities of one and two electron ions under strongly coupled plasma. *Phys. Plasmas* **2013**, *20*, 013505.
35. Sen, S.; Mandal, P.; Mukherjee, P.K. Positronium formation in positron-helium collisions with a screened Coulomb interaction. *Eur. Phys. J. D* **2012**, *66*, 230–241.
36. Montgomery, H.E., Jr.; Sen, K.D. Dipole polarizabilities for a hydrogen atom confined in a penetrable sphere. *Phys. Lett. A* **2012**, *376*, 1992–1996.
37. Ichimaru, S.; Strongly coupled plasmas: High-density and degenerate electron liquids. *Rev. Mod. Phys.* **1982**, *54*, 1017–1059.
38. Lai, H.F.; Lin, Y.C; Ho, Y.K. Two-photon transitions in the He^+ ion embedded in strongly-coupled plasmas. *J. Phys. Conf. Ser.* **2009**, *163*, 012096.
39. Ho, Y.K.; Lai, H.F.; Lin, Y.C. Two-photon 1s-3d and 1s-4d transitions in the He^+ ion embedded in strongly-coupled plasmas with ion-sphere model. *J. Phys. Conf. Ser.* **2009**, *194*, 022023.
40. Nascimento, E.M.; Prudente, F.V.; Guimarães, M.N.; Maniero, A.M. A study of the electron structure of endohedrally confined atoms using a model potential. *J. Phys. B At. Mol. Opt. Phys.* **2011**, *44*, 1–7.
41. Quattropani, A.; Bassani, F.; Carillo, S. Two-photon transitions to excited states in atomic hydrogen. *Phys. Rev. A* **1982**, *25*, 3079–3089.
42. Tung, J.H.; Ye, X.M.; Salamo, G.J.; Chan, F.T. Two-photon decay of hydrogenic atoms. *Phys. Rev. A* **1984**, *30*, 1175–1184.
43. Bhatti, M.I.; Perger, W.F. Solutions of the radial Dirac equation in a B-polynomial basis. *J. Phys. B At. Mol. Opt. Phys.* **2006**, *39*, 553–558.
44. Bhatta, D.D.; Bhatti, M.I. Numerical solution of KdV equation using modified Bernstein polynomials. *Appl. Math. Comput.* **2006**, *174*, 1255–1268.
45. Paul, S.; Ho, Y.K. Two-photon transitions in hydrogen atoms embedded in weakly coupled plasmas. *Phys. Plasmas* **2008**, *15*, 1–7.
46. Lumb, S.; Lumb, S.; Prasad, V. Multi-photon transitions in confined atoms. **2016**, in preparation.